Online Adaptive Geometry Predictor of Aquaculture Fish-Nets

Svetlana Potyagaylo and Savvas G. Loizou

Abstract— **This paper proposes an online adaptive geometry predictor for aquaculture fish-nets. The 3D fish-net model is based on a lumped-mass method according to which the net meshes are represented by four interconnected cylindrical elements. The external forces are applied at the center of each element, while the internal forces are calculated as tension forces between two neighboring mass points. The model is validated through several simulations for a small-scale open cylinder exposed to steady uniform current. The preliminary simulation results of the full aquaculture net system are provided as well. The proposed predictor will be used as an information source in the control architecture of an underwater vehicle.**

I. INTRODUCTION

In the recent years, underwater remotely operated vehicles (ROVs) have become an important tool in different undersea applications, especially within the aquaculture industry to inspect and monitor fish cage systems. The fish cage systems consist of net cages, mooring ropes, floating collar structures, sinkers and anchors. Regular inspection of all subsystems and early detection of net holes and other types of system faults are mandatory tasks in the fish production industry. Currently, such operations are provided by human divers. However, due to the environmental and aesthetic aspects of near-shore fish farm locations, more fish cage systems have moved to offshore sites with more severe waves and currents [1], [2]. In this case, ROVs appear to be a safe and cost-efficient alternative to the human diving inspection by avoiding the health and human life risks.

The current work is an ongoing research project aimed to develop an autonomous system for visual inspection of fish farm nets and moorings by using a tethered underwater robotic vehicle. In order to inspect and monitor the aquaculture system, the vehicle has to execute different tasks, such as localization, path and motion planning, fish net tracking, and stabilization near the location of interest. The GPS-denied undersea environments make the autonomous operation of underwater ROVs to be one of the most challenging problem. The effective and accurate localization and control is enabled by a fusion of onboard sensor information and a-priory knowledge about dynamic behaviour of the aquaculture net system as well of the ROV itself.

A fish net is a dynamic flexible structure that depends on sea currents and waves. Recently, extensive theoretical and numerical investigations have been carried out to model the hydrodynamic response of net cages. Aarsnes et al. [3] were among the first that conducted theoretical studies to calculate forces acting on the net panel and experiments to determine the net-current interaction and velocity reduction within net cage systems. Tsukrov et al. [4] proposed a consistent finite element method to model the hydrodynamic response of net panels. They verified the model through experiments in the steady flow. Lader et al. [5] developed a dynamic model for 3D net structures exposed to waves and current. They divided the net structure into square super-elements for which the hydrodynamic forces were calculated. In the proposed model, each node of the super-element was connected to others by nonlinear springs that produced the structural forces. Zhao et al. [6] proposed a numerical model based on a lumped-mass method. They conducted experiments and provided comparison with other approaches as well. Huang et al. [7] developed a numerical model to analyze the dynamic behavior of a net-cage system in currents. In this model, the net cage was divided into plane surface elements on which the hydrodynamic forces were calculated. The comparison between the numerical and experimental results were provided to estimate the net volume reduction.

The purpose of the current study is to develop an adaptive aquaculture fish-net geometry predictor, that is, a numerical model of the aquaculture net cage appropriate for implementation in the motion planning and control architecture of an inspection ROV. The netting structure is the largest part of fisheries and experiences significant deformations caused by offshore currents. Moe et al. [8] showed that the net volume reduction is proportional to the current velocity and may be up to 70% in water currents with velocity 0.1-0.5m/s. In return, the net structure influences the flow around the cage as well. Klebert et al. [1] proposed a comprehensive review of research works on flow hydrodynamics within and around a single net cage and a cage array. The theoretical and experimental results of flow reduction caused by a number of factors, such as net solidity, cage design and biological effect of fish are represented in the review as well.

The rest of the paper is organized as follows: Section II gives a description of the proposed methodology along with a fish cage numerical model. Section III describes a method for adaptive online prediction of the net geometry. Section IV provides the simulation results of a small-scale net model in comparison with the experimental results of other research works. Section V concludes the paper and contains the description of future work.

This work was supported by the Cyprus Research Promotion Foundation under grant ΑΕΙΦΟΡΙΑ/ΓΕΩΡΓΟ/0311(BIE)/08

The authors are with the Mechanical and Materials Science and Engineering Department, Cyprus University of Technology, Limassol 3041, CYPRUS, {svetlana.potyagaylo, savvas.loizou}@cut.ac.cy

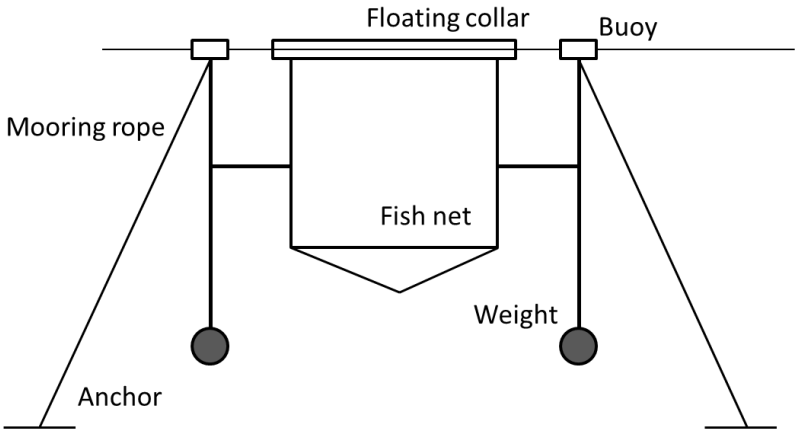

Fig. 1. An example of a fish cage system.

II. METHODOLOGY

A. Model Description

In this work, we assume a "gravity" net cage system that consists of a floating collar, a netting system, weights, mooring ropes and anchors. The schematic diagram of such a system is shown in Figure 1. The "lumped-mass method" concept is used here to model a fish net structure. According to this concept, the net is divided into discrete net elements with lumped masses at the element nodes connected by massless springs as depicted in Figure 2. In this case, each net mesh represents a structure of four interconnected bars that are subject to the external forces applied at the center of the element. The internal (structural) forces are incorporated into the model as well in order to address the flexibility of the net structure.

We assume that the mesh bar is cylindrical, so the lumped mass point at each end of the mesh bar has the dynamic characteristics of corresponding cylindrical elements. The coordinates of each point define the net shape for the given boundary and flow conditions. In addition, we assume that the cross-section area of the mesh bars remains constant and the internal forces are applied only along the bars.

B. External Forces Acting on a Net Element

The resulting force on a moving body in an unsteady viscous flow can be determined using Morrison equation, which is a combination of an inertial term and a drag term:

$$\mathbf{F} = \mathbf{F}_D + \mathbf{F}_I, \tag{1}$$

where $\mathbf{F}_D = \frac{1}{2}\rho C_D A \mathbf{U}_R \left|\mathbf{U}_R\right|$ is the drag force, and $\mathbf{F}_I = \rho C_a V \dot{\mathbf{U}}_R + \rho V \dot{\mathbf{U}}$ is the inertia force.

Here ρ is the water density, C_D is the drag coefficient, A is the reference area (an area of the body perpendicular to the flow), $\mathbf{U}_R = \mathbf{U} - \mathbf{V}$ is the relative flow velocity, $\mathbf{U}$ is the flow velocity, $\mathbf{V}$ is the body velocity, C_a is the added mass coefficient, V is the body volume. Bold letters denote vectors.

In order to model the full dynamics of a body in the fluid environment, the gravitational force and the buoyancy force should be included as well. These forces may be expressed as:

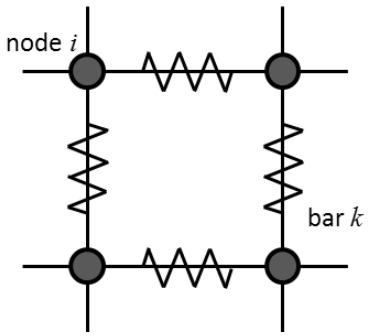

Fig. 2. A schematic diagram of a lumped-mass model.

$$\begin{aligned} \mathbf{F}_G &= M\mathbf{g}, \\ \mathbf{F}_B &= (\rho - \rho_b) V \mathbf{g}, \end{aligned} \tag{2}$$

where M is the body mass, $\mathbf{g}$ is the gravitational constant vector, ρ_b is the body density.

In this work, we use cylindrical bar elements. The drag force acting on a such element may be divided into two components: the normal component and the tangential component, relative to the bar [9]. These forces can be represented as follows:

$$\begin{aligned} \mathbf{F}_n &= \frac{1}{2}\rho C_n A \left|\mathbf{U}_{Rn}\right|^2 \mathbf{e}_n, \\ \mathbf{F}_t &= \frac{1}{2}\rho C_t A \left|\mathbf{U}_{Rt}\right|^2 \mathbf{e}_t, \end{aligned} \tag{3}$$

where $A = dl$ is a cross-sectional area of the bar element, d is the element diameter which is the same as the twine thickness, l is the length of the bar element, C_n and C_n are the normal and tangential drag coefficients, $\mathbf{U}_{Rn}$ and $\mathbf{U}_{Rt}$ are the normal and tangential relative velocity components, $\mathbf{e}_n$ and $\mathbf{e}_t$ are the unit vectors in the normal and tangential directions, respectively.

The drag coefficients are functions of the Reynolds number and may be calculated using the following expres-

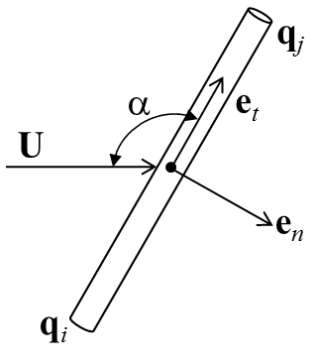

Fig. 3. Normal and tangential unit vectors and angle of attack definitions.

sions [10]:

$$C_n = \begin{cases} \frac{8\pi}{Res}\left(1 - 0.87s^{-2}\right) & \text{if } 0 < Re \leq 1, \\ 1.45 + 8.55Re^{-0.9} & \text{if } 1 < Re \leq 30, \\ 1.1 + 4Re^{-0.5} & \text{if } 30 < Re \leq 10^5, \end{cases} \qquad (4)$$
$$C_t = \pi\mu\left(0.55Re^{0.5} + 0.084Re^{2/3}\right),$$

where $Re = \frac{\rho \mathbf{U}_{Rn} d}{\mu}$ is the Reynolds number, μ is the water viscosity, $s = -0.077215665 + \ln(8/Re)$.

The normal and tangential unit vectors may be found as [9]:

$$\mathbf{e}_n = \frac{\mathbf{e}_{bar} \times (\mathbf{U}_R \times \mathbf{e}_{bar})}{|\mathbf{e}_{bar} \times (\mathbf{U}_R \times \mathbf{e}_{bar})|}, \qquad (5)$$
$$\mathbf{e}_t = \frac{\mathbf{e}_n \times (\mathbf{U}_R \times \mathbf{e}_n)}{|\mathbf{e}_n \times (\mathbf{U}_R \times \mathbf{e}_n)|},$$

where $\mathbf{e}_{bar} = \frac{\mathbf{q}_i - \mathbf{q}_j}{|\mathbf{q}_i - \mathbf{q}_j|}$ is the bar unit vector, $\mathbf{q}_i$ and $\mathbf{q}_j$ is the coordinate vector of two neighboring mass points as shown in Figure 3.

The normal and tangential velocity components are calculated as:

$$\mathbf{U}_{Rn} = \mathbf{U}_R \sin\alpha, \qquad (6)$$
$$\mathbf{U}_{Rt} = \mathbf{U}_R \cos\alpha,$$

where α is the angle of attack defined as an angle between the flow velocity direction and the normal to the net element.

C. Internal Forces Acting on a Net Element

The flexibility of the net structure can be described by elastic (tension) forces of the twines. We assumed that the net element nodes are connected through massless springs, so each node is subject to four elastic forces from the neighboring nodes. The force in the spring between nodes i and j is given by (Figure 4):

$$\mathbf{F}_E^{ij} = \sigma_{ij}\mathbf{e}_{bar}^{ij}, \qquad (7)$$

where σ_{ij} is the force magnitude, and $\mathbf{e}_{bar}^{ij}$ is the bar unit vector.

The force magnitude (tension) may be expressed as:

$$\sigma_{ij} = \begin{cases} C_1\varepsilon_{ij} & \text{if } \varepsilon_{ij} > 0, \\ 0 & \text{if } \varepsilon_{ij} \leq 0, \end{cases} \qquad (8)$$

where C_1 is the elastic coefficient of the twine, ε_{ij} is the elongation of the spring ij:

$$\varepsilon_{ij} = \frac{l_{ij} - l_{ij}^0}{l_{ij}^0}. \qquad (9)$$

Here l_{ij}^0 is the undeformed length between the nodes i and j, l_{ij} is the deformed length between these two nodes. If the position of the nodes i and j is defined by vectors $\mathbf{q}_i$ and $\mathbf{q}_j$, respectively, the deformed length between the nodes is calculated as follows:

$$l_{ij} = |\mathbf{q}_i - \mathbf{q}_j|. \qquad (10)$$

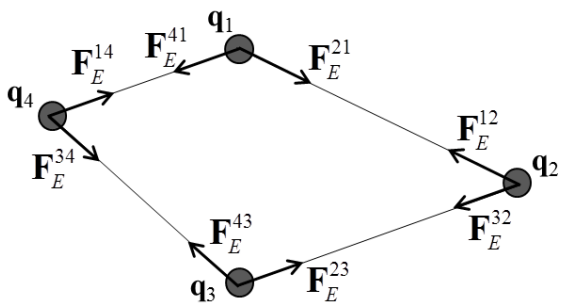

Fig. 4. The structural forces of mesh bar elements.

D. Motion Equations of a Net Structure

The motion of a net structure may be represented by the motion of its mass points under external and structural forces. Substituting the equations Eq. (2), Eq. (3) and Eq. (7) in Eq. (1) and applying the Newton's law, we get the following motion equation for each lumped mass point i:

$$(m_i + \Delta m_i)\frac{\partial^2 \mathbf{q}_i}{\partial t^2} = \mathbf{F}_i^{ext} + \mathbf{F}_i^{int}. \qquad (11)$$

We assume a steady current flow, so the inertial force is equal to zero: $\mathbf{F}_I = 0$. The external forces $\mathbf{F}^{ext}$ and the internal force $\mathbf{F}^{int}$ are calculated for each bar k and then uniformly distributed to the corresponding mass points. For each point, the applied forces will be as follows:

$$\mathbf{F}_i^{ext} = \frac{1}{2}\sum_{k=1}^{4}\left(\mathbf{F}_n^k + \mathbf{F}_t^k\right) + \mathbf{F}_{Gi} + \mathbf{F}_{Bi}, \qquad (12)$$
$$\mathbf{F}_i^{int} = \mathbf{F}_E^{i,i-1} + \mathbf{F}_E^{i,i+1},$$

where m_i is the mass of the point i, $\Delta m_i = \rho C_a V$ is the added mass of the point i, k the index of corresponding bar elements. The distribution of the forces acting on the point i is shown in Figure 5.

The resulting system of equations is non-linear with $N \times 3$ unknown mass point coordinates and may be solved using an iterative numerical method. We applied the Newton-Raphson

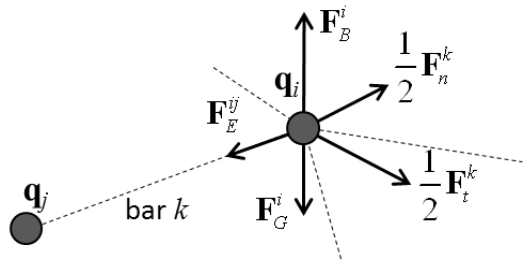

Fig. 5. The force distribution for a mass point i.

iterative method as a common scheme for finding solutions of non-linear systems. However, the convergence issues should be taken into account during the choice of the numerical method. When the number of net bar elements grows, the length of each element and distances between mass points decrease. In this case, the system becomes multi-degree-of-freedom and may have multiple local minima. This can cause the iterative process to converge to one of the local minima or to diverge.

This problem may be resolved by applying the time integration scheme of the Runge-Kutta algorithm, for instance. However, this process may be time-consuming as well because for more accurate discretization of the netting, the integration step size should be relatively small.

III. ONLINE ADAPTIVE PREDICTION OF FISH NET GEOMETRY

As was described earlier, inspection of the fish net and mooring system integrity and timely detection of faults is especially important task in fish aquaculture farming. In order to fulfil this task in an automatic manner, a ROV should be capable to navigate to a target (net cage or mooring system), to localize it and stabilize itself at a predefined distance from the target. For this purpose, a laser vision system, similar to one developed by Karras and Kyriakopoulos [11] but with appropriate modifications may be used. This system consists of a camera and laser pointers that project dots on the target surface. The laser dots can be tracked by the camera, so the distance between the ROV and the target can be estimated. Based on information of its position, the ROV can evaluate the laser dot coordinates and the net geometry.

The developed numerical model of the net cage system is used off-line to provide a priori known information about the net cage for different current conditions. This information may be updated online when the new estimation of the net geometry becomes available. Since the laser vision system of the ROV can observe only a limited area of the cage system and estimate the coordinates of the several net knots, the resolving of the net model is required. However, in comparison with the off-line solution that is found by the time-consuming integration scheme with zero initial conditions, the new solution of the system can be obtained faster. In general, the flow velocity changes relative slowly. Therefore, in the online regime we have a good prediction of the net geometry that may serve as an initial guess. Since there is a strong relationship between the current velocity and the net shape, the discrepancy between the predicted and actual net positions may be caused by changes in the flow speed. An adaption rule has been developed by considering the coordinate discrepancy as a residual function required to be vanished. Then, the new current velocity and the net geometry can be evaluated using the Newton-Raphson algorithm:

$$\mathbf{U}_{new} = \mathbf{U}_{old} - \frac{f\left(\mathbf{U}_{old}\right)}{f'\left(\mathbf{U}_{old}\right)}, \tag{13}$$

where $f = \mathbf{q}_{old} - \mathbf{q}_{new}$ is the residual function between the old position of the net node predicted offline and the new node position estimated by the laser vision system.

IV. SIMULATION RESULTS

A. Validation results

The developed numerical model was validated through simulations and comparison with experiments made by Lader and Enerhaug [12]. The input data are listed in Table I. In this model test, the net has a form of an open cylinder which top is mounted to the fixed hoop. Sixteen weights with the mass of 400 g were positioned uniformly along the circumference of the cylinder bottom.

TABLE I
THE MAIN INPUT PARAMETERS.

Parameter	Value
Cylinder diameter D, [m]	1.435
Cylinder height h, [m]	1.435
Net twine thickness d_{tw}, [mm]	1.8
Twine density ρ_{tw}, [kg/m^3]	1130
Twine elastic coefficient C_1, [N/m^2]	784.9×10^6

The net configuration used for model validation is shown in Figure 6. The model was tested for six current velocities: $|\mathbf{U}|$ = 0.04, 0.13, 0.21, 0.26, 0.33 and 0.52 m/s that were applied along the X-axis direction.

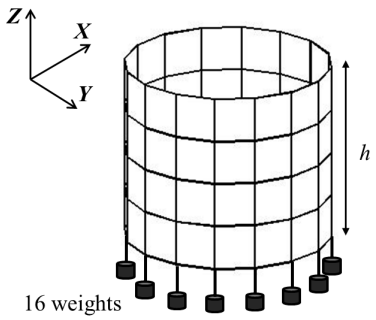

Fig. 6. A net model used in simulations.

As in the work of Lader et al. [12], the net cylinder was divided into sixteen elements around the circumference and four elements along the Z-axis. The total number of the mass points was 80.

The simulation results of the deformed net structure exposed to the current are shown in Figure 7. The calculated

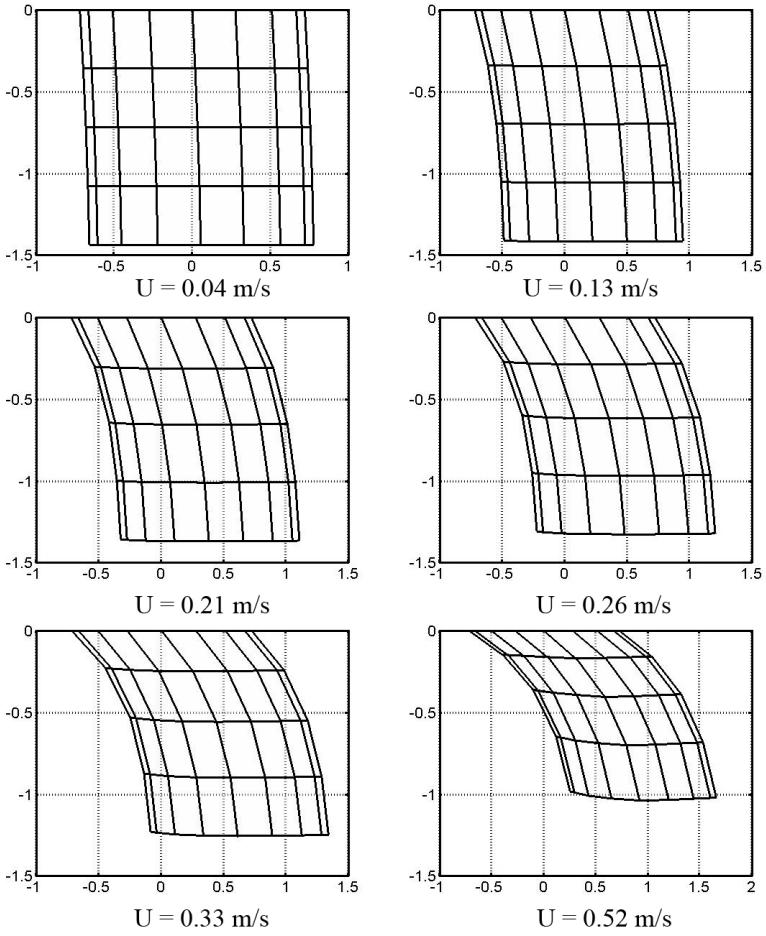

Fig. 7. Simulation results of the fish net structure for different current velocities.

total drag force compared with the drag force measured in the experiments of Lader et al. [12] for each velocity case is shown in Figure 8. The results show a good agreement between the Lader's experiments and the proposed model, especially for the small current velocities. The model was also compared with numerical models of Zhao et al. [6] and Huang et al. [7] that conducted the simulations and experiments with a similar net structure.

B. Simulation of a full fish-net system

The numerical model was tested for a full fish-net system that is shown in Figure 1. In this case, we used a model of the net structure described in Section II. The net has a form of a cylinder tapered at the bottom. In addition, the mooring structure that consists of mooring ropes and a system of weights was modeled as well. The mooring ropes were assumed to be cylindrical and were also modeled as bar elements with mass points at the ends. The main geometric parameters of the system and material properties are listed in Table II.

Figure 9 shows the shape of the net cage system exposed to the current of 0.2 m/s. The top of the netting and of the mooring ropes were fixed. In the presence of the mooring rope and the system of weights, the changes of the net position are smaller compared to the open cylinder simulation results.

TABLE II

THE MAIN PARAMETERS OF A NET CAGE SYSTEM.

Parameter	Value
Net diameter, [m]	2
Cylinder height, [m]	1.6
Cone height, [m]	0.5
Net twine thickness, [mm]	1.8
Twine density, [kg/m^3]	1130
Twine elastic coefficient, [N/m^2]	345.37×10^6
Rope thickness,[mm]	50
Rope elastic coefficient, [N/m^2]	784.9×10^6

C. Simulation results of online predictive method

The method for online adaptive prediction of fish-net geometry described in Section III were validated in simulation as well. Figure 10 shows the value of the residual function and the number of iterations required to estimate a new net position since the current velocity has decreased by 0.1 m/s. The Newton-Raphson algorithm for solving nonlinear

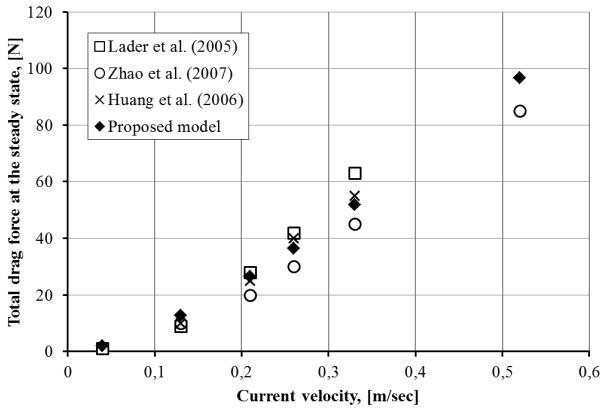

Fig. 8. The comparison of the total drag force with other research works (Huang et al. [7], Lader et al. [12], Zhao et al. [6]).

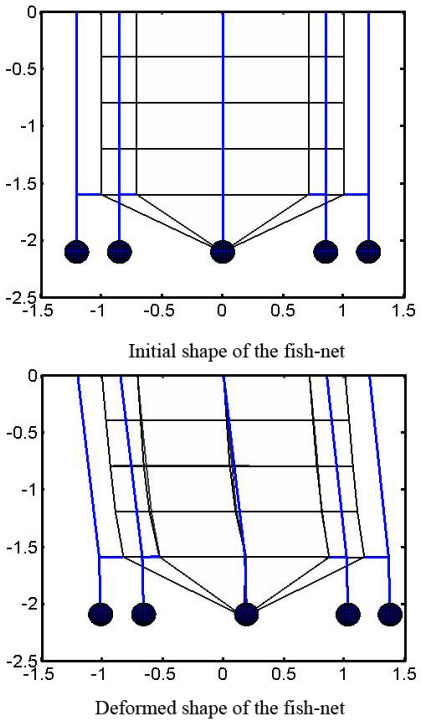

Fig. 9. Simulation results of the full aquaculture fish-net structure.

systems was used here and the required time was approximately 30-40 second. The simulations were conducted using MATLAB® and an Intel Pentium Core2 2.83 GHz processor with a 3.25 GB RAM.

V. CONCLUSIONS AND FUTURE WORK

This paper presents a numerical model of an aquaculture cage system exposed to ocean uniform current. This model is based on a lumped-mass approach. The net structure and the mooring ropes of the cage system were divided into a set of mass points connected by cylindrical bar elements. This model was validated through a series of simulations and compared with experiments described in other research works.

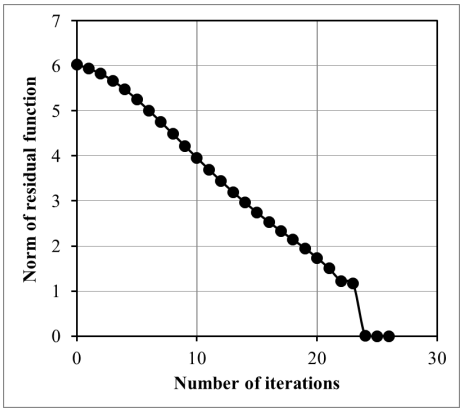

Fig. 10. The residual norm as a function of the iteration number for the current velocity updating.

This paper represents an ongoing project aimed to develop an autonomous robotic system for fish farming inspection. The presented results are preliminary results of the control architecture development for an underwater vehicle. The control system will utilize information from different sources, including online adaptive prediction of the fish net geometry. As the future work, we will also consider the implementation issues for decreasing the computational costs of the proposed algorithms, such as using the optimized program code.

REFERENCES

[1] P. Klebert, P. Lader, L. Gansel, and F. Oppedal, "Hydrodynamic Interactions on Net Panel and Aquaculture Fish Cages: A Review," *IEEE Journal of Ocean Engineering*, vol. 58, pp. 260–274, 2013.

[2] Y.-P. Zhao, T.-J. Xu, C.-W. Bi, G.-H. Dong, and S.-C. Liu, "The Numerical Simulation of Hydrodynamics of Fishing Net Cage," *Hydrodynamics - Theory and Model*, 2012.

[3] J. Aarsnes, H. Rudi, and G. Loland, "Current forces on cage, net deflection," *Engineering for Offshore Fish Farming*, pp. 137–152, 1990.

[4] D. W. Fredriksson, M. R. Swift, J. D. Irish, I. Tsukrov, and B. Celikkol, "Fish Cage and Mooring System Dynamics Using Physical and Numerical Models with Field Measurements," *Ocean Engineering*, vol. 30, pp. 251–270, 2003.

[5] P. F. Lader, B. Enerhaug, A. Fredheim, and J. Krokstad, "Modelling of 3D Net Structures Exposed to Waves and Current," in *International Conference on Hydroelasticity in Marine Technology*, 2003.

[6] Y.-P. Zhao, Y.-C. Li, G.-H. Dong, F.-K. Gui, and B. Teng, "Numerical Simulation of the Effects of Structure Size Ratio and Mesh Type on Three-Dimensional Deformation of the Fishing-Net Gravity Cage in Current," *Aquacultural Engineering*, vol. 36, pp. 285–301, 2007.

[7] C.-C. Huang, H.-J. Tang, and J.-Y. Liu, "Dynamic Analysis of Net Cage Structures for Marine Aquaculture: Numerical Simulaion and Model Testing," *Aquacultural Engineering*, vol. 35, pp. 258–270, 2006.

[8] H. Moe, A. Fredheim, and O. Hopperstad, "Structural Analysis of Aquaculture Net Cages in Current," *Journal of Fluids and Structures*, vol. 26, no. 3, pp. 503–516, 2010.

[9] D. Priour, *A Finite Element Method for Netting: Application to Fish Cages and Fishing Gear*. Springer Briefs in Environmental Science, Springer, 2013.

[10] Y.-I. Choo and M. J. Casarella, "Hydrodynamic Resistance of Towed Cables," *Journal of Hydronautics*, vol. 5, no. 4, pp. 126–131, 1971.

[11] G. C. Karras and K. J. Kyriakopoulos, "Localization of an Underwater Vehicle using an IMU and a Laser-based Vision System," in *Mediterranean Conference on Control and Automation*, 2007.

[12] P. F. Lader and B. Enerhaug, "Experimental Investigation of Forces and Geometry of a Net Cage in Uniform Flow," *IEEE Journal of Ocean Engineering*, vol. 30, no. 1, pp. 79–84, 2005.